Analyst

Interdisciplinary detection science

www.rsc.org/analyst

Volume 136 | Number 2 | 21 January 2011 | Pages 213–416

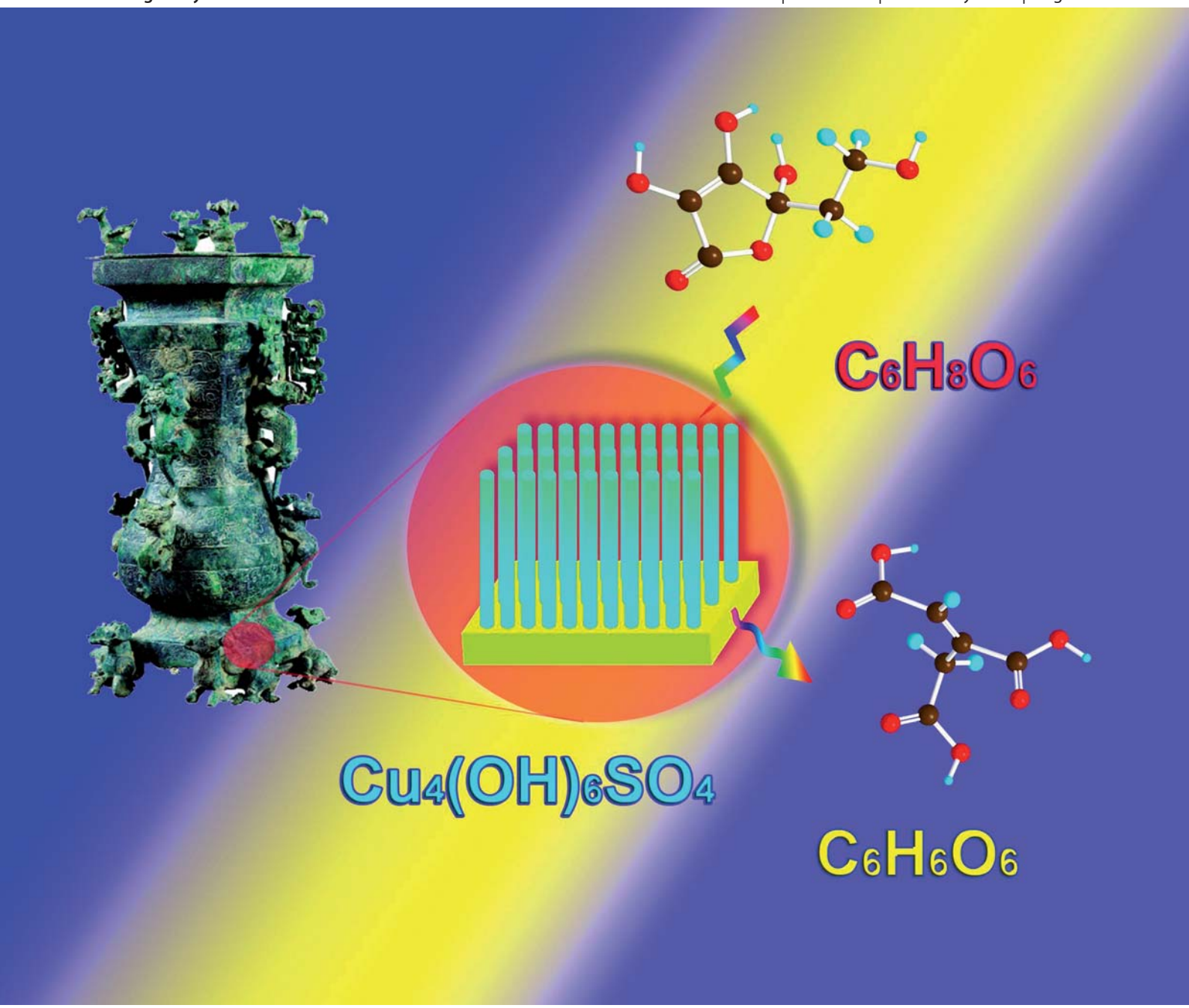

ISSN 0003-2654

RSC Publishing

COMMUNICATION

Cao Xia and Wang Ning

A novel bio-electrochemical ascorbic acid sensor modified with $Cu_4(OH)_6SO_4$ nanorods

A novel bio-electrochemical ascorbic acid sensor modified with $Cu_4(OH)_6SO_4$ nanorods

Cao Xia[ab] and Wang Ning*[b]

Received 18th June 2010, Accepted 27th September 2010
DOI: 10.1039/c0an00416b

$Cu_4(OH)_6SO_4$ (brochantite) is an undesirable oxidation product of copper-bearing sulfides, and it is seldom considered to be biologically and electrochemically active. In this paper, we report that $Cu_4(OH)_6SO_4$ nanoparticles in fact possess an intrinsic electrocatalytic activity, which is explored as a biosensing material to oxidize L-ascorbic acid (AA). The $Cu_4(OH)_6SO_4$ nanorod modified biosensor exhibits excellent performance for the determination of L-ascorbic acid with a response time of less than 8 s, a linear range between 0.017 and 6 mM, and a sensitivity of 17.53 μA mM^{-1}. A high selectivity towards the oxidation of AA in the presence of dopamine (DA) and acetyl aminophenol (AP) is also observed at their maximum physiological concentrations. The good analytical performance and long-term stability, low cost and straightforward fabrication method made the $Cu_4(OH)_6SO_4$ nanomaterials promising for the development of effective electrochemical sensors for a wide range of potential applications in medicine, biotechnology and environmental chemistry.

Introduction

L-Ascorbic acid (AA) is a powerful antioxidant present in food and beverages, and it is also used as a marker chemical in evaluating food deterioration and product quality.[1] The determination of AA has attracted great attention in biomedical engineering, food and pharmaceutical industries. As a result, developing convenient and rapid electrochemical procedures for measuring AA levels has been the subject of considerable interest both for food and pharmaceutical quality and safety.[2–16]

Now many researchers are trying to make the dream of direct electrochemical determination of AA concentration come true, and their interest in practical non-enzymatic AA sensors has been centered on the efforts to find out the breakthrough in electrocatalysis.[6,7] Screening suitable catalysts of both high selectivity and activity can be not only of great scientific significance, but also could produce real benefits for the above-mentioned practical applications. However, at present, such electrochemical catalysts still need to face the difficulties such as low stability and activity.[7,8] In addition, other electroactive species such as dopamine (DA) and acetyl aminophenol (AP) usually coexist with AA in the central nervous system. Because the oxidation potentials of AP and DA are rather close to AA, their signal separation is rather difficult, even at noble metal-based electrodes, which are generally considered as ideal catalysts of high efficiency. The successful sensing of AA with high efficiency and selectivity from DA and AP is still a major challenge to electrochemical scientists.[8–16]

In the past several years, various techniques, such as noble metals,[6] C_{60} film,[9] carbon nanotube composite films,[10–13] and covalently modified polymers[14–16] have been successfully employed for the smart detection of AA in the presence of other interferents. Recently, endeavors have also been taken in the direction of transition metal compound-based cheap catalysts for the successful separation of the voltammetric peaks of AA from those of DA and AP.[7] In this case, though often suffering from very low surface areas and poor catalytic efficiency, transitional metal-based compounds represent a great advantage for the development of large-scale and low-cost electrochemical sensors for practical use without any possible oxygen limitation, thermal or chemical deformation during sensor fabrication, storage and use.

Natural copper hydroxysulfates are mainly formed by the oxidation of copper-bearing sulfides, and the key feature of their structure is the presence of edge-shared copper octahedra.[17,18] In the past, $Cu_4(OH)_6SO_4$ has generally been thought to be an undesirable oxidation product of copper-bearing sulfides and has seldom been considered to be biologically and electrochemically active. However, from a positive point of view, the $Cu_4(OH)_6SO_4$ nanoparticles on the electrode surface may also mediate the final heterogeneous chemical oxidation or reduction of the target materials while the converted copper ions can be continuously recovered by electrochemical oxidation or reduction. It is these reasons that stimulated our interest for the synthesis, structural characterization, and studies of the electrocatalytic properties of copper hydroxysulfates.

In this paper, brochantite nanorods were first synthesized by a mild wet chemical method. An electrochemical AA electrode was then fabricated and electrochemically characterized based on the modification of such copper nanomaterials. It is surprising to discover that brochantite nanoparticles in fact possess an intrinsic electrocatalytic activity. The high catalytic activity and excellent selectivity toward the oxidation of AA, DA and AP may contribute to their diverse, promising applications in biosensors, electroanalysis, as well as other electro-releasing devices.

[a]*School of Material Science and Engineering, Jiangsu University of Science and Technology, Jiangsu, 212003, China*
[b]*School of Chemistry and Environment, Beijing University of Aeronautics and Astronautics, Beijing, 100083, China. E-mail: wangning@buaa.edu.cn; Fax: +86-10-82338162; Tel: +86-10-82338162*

Experimental

Brochantite nanorods were synthesized as the following process. In brief, 1.2 g of copper chloride ($CuCl_2 \cdot 2H_2O$), 6 g of poly(vinyl pyrrolidone) (PVP, MW 30 000), 10 g of NH_4SO_4 and 2 g of NaOH were dissolved 150 mL of pure water to form a green solution by ultrasonication for 30 min. The mixture was stirred vigorously and refluxed for 12 h, and the green powder was taken out and washed with ethanol and water for several times, then dried in air for characterization. The brochantite nanorods modified electrode (NBE) was prepared using a co-precipitation method.[19] In addition, a bulk brochantite modified electrode (BBE) was also prepared for comparison.

Scanning electron microscopy images were obtained by employing a Hitachi S4800 cold field emission scanning electron microscope (CFE-SEM). An X-ray powder diffraction (XRD) pattern of the corrosion products was collected by a Rigaku X-ray diffractometer (Rigaku Goniometer PMG-A2, CN2155D2, wavelength = 0.15147 nm) with Cu Kα radiation. All the electrochemical tests were carried out at room temperature under a nitrogen atmosphere on a CHI 660C electrochemical station, using a single compartment, three-electrode cell. Electrode potentials were measured with respect to an aqueous saturated calomel electrode (SCE). A Pt wire was used as the counter electrode.

Results and discussion

Fig. 1 shows the X-ray diffraction (XRD) pattern of the as-prepared powder. All the reflection peaks of the products can be indexed as standard monoclinic brochantite (*P*21/*a*(14), JCPDS 43-1458), confirming the pure phase of brochantite $Cu_4(OH)_6SO_4$. No characteristic diffraction peaks from other phases or impurities were detected.

As can be seen from Fig. 2, the product is made up of nanorods with an average length of 1–2 μm and diameter of about 80–100 nm. *Generally, size and shape of the nanorods mainly determines their specific surface related properties. In most of the applications, the catalytic performance is strongly dependent on the particle size, and nanoparticles with a smaller size will show a higher specific area and thus a higher catalytic performance and sensitivity.* Cherishing the merits of high specific area and structural stability, the brochantite nanorods modified electrode (NBE) surface may both limit the denaturing adsorption to a lesser extent and induce the adsorbed molecules in a more favorable orientation and conformation for rapid electron transfer. Thus the NBE electrode may display improved electrocatalytic performance.

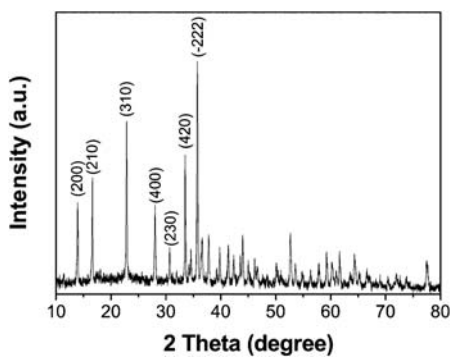

Fig. 1 XRD pattern of the as-synthesized $Cu_4(OH)_6SO_4$ (the peaks are too dense to be indexed one by one).

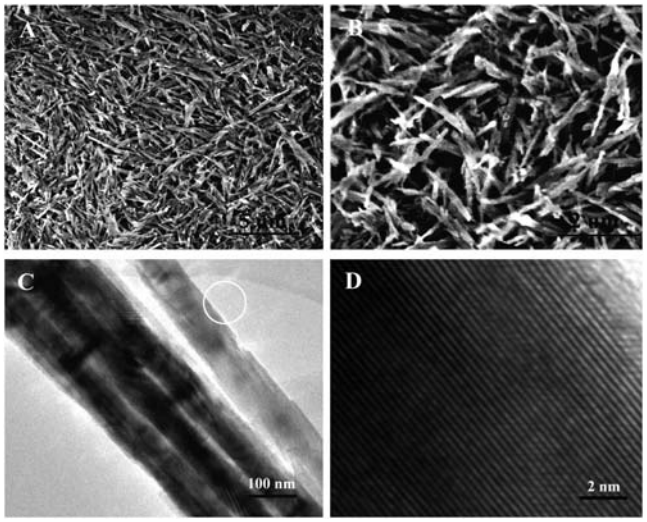

Fig. 2 SEM images of the as-synthesized $Cu_4(OH)_6SO_4$.

Cyclic voltammograms (CVs) were recorded to understand the electrocatalytic behavior of the NBE electrode in 0.1 M PBS solutions towards the oxidation of 0.5 mM AA at a scan rate of 0.1 V s^{-1}. As can be clearly witnessed from Fig. 3, the NBE electrode showed pronounced electrocatalytic effect for the oxidation of AA in comparison to the BBE electrode. This is proved by the greatly enhanced peak currents for the oxidation of AA with an oxidation potential of −0.017 V, which was far less than that with the BBE electrode (0.207 V). However, the CVs of the NBE electrode run in a blank PBS solution (containing no AA) did not show any peaks. Meanwhile, almost no peak current decay was observed on the NBE electrode after repetitive potential scan for 20 cycles at the same solutions. Thus

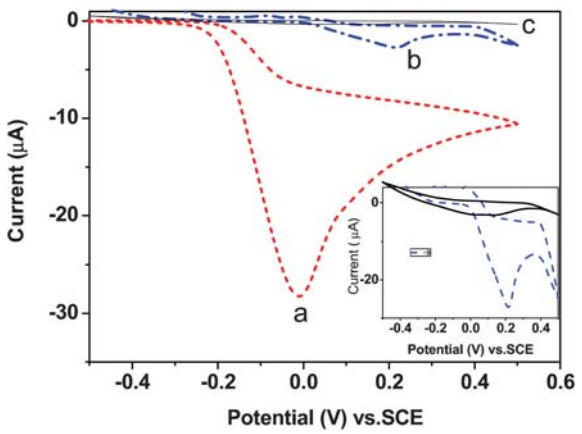

Fig. 3 Cyclic voltammograms of the NBE electrode in 0.1 M phosphate buffer solutions (PBS, pH = 7.7) containing 0.5 mM AA at scan rate of 0.1 V s^{-1}: (a) NBE electrode; (b) BBE electrode; (c) NBE electrode in the absence of AA; the inset is the magnification of curves (b) and (c).

it can be deduced that little nano $Cu_4(OH)_6SO_4$ powder was peeled off from the electrode surface.

In the potential range within which the Cu(II)/Cu(I) centers can be involved in a redox process, the material displays good conductivity due to the electronic and ionic transport.[20] The oxidation process can be deduced through an electrocatalytic mechanism involving the Cu(II)/Cu(I) centers, and the catalytic mechanism of the $Cu_4(OH)_6SO_4$ to AA oxidation can be explained by the following scheme:

$$2Cu(II) + C_6H_8O_6 + H_2O \rightarrow Cu(I) + 2H^+ + C_6H_6O_6 \quad (1)$$

$$2Cu(I) \rightarrow 2Cu(II) + 2e \quad (2)$$

The pH of the supporting electrolyte has a significant influence on the AA electro-oxidation at the NBE electrode by affecting both the peak current and peak potential. Fig. 4A shows the CVs of the NBE in 0.5 mM AA with different pH values, and Fig. 4B illustrates the dependence of the AA anodic peak current and redox potential on the buffer solution pH. The anodic peak current increased with increasing solution pH, while the AA peak current peaked at pH 7.7. In addition, the anodic peak potentials for the oxidation of AA shifted towards the negative direction with increasing pH, showing that protons have taken part in their electrode processes. Plots of redox potential *versus* pH for the NBE electrode were linear in the pH range from 5.5 to 8.5, as shown in Fig. 4B. Slopes in this pH range were −64 mV/pH which is close to the theoretical value of −60 mV/pH for a $2e^-/2H^+$ redox process. For the ternary mixture containing AA, phosphate buffer was used to control the pH of the mixture and the pH value of 7.7 was chosen, which is much closer to physical conditions, and at this pH the oxidations of AA have high electrochemical response.

Kinetic and transport characteristics of the NBE electrode were investigated by performing cyclic voltammetry experiments with different scan rates. Fig. 5A shows the CVs of the NBE electrode in 0.1 M PBS solutions containing 0.5 mM AA at different scan rates (0.01 to 0.1 V s^{-1}). It is interesting to note that the oxidation peak potential (E_{ap}) for AA shifts positively when increasing the scan rates, indicating a kinetic control over the oxidation of AA at the redox sites of the NBE electrode. A Tafel slope of 63 mV was obtained based on the slope of the linear plot (E_{ap} *vs.* log *V*) for the NBE electrode. This slope indicates the fact that a two-electron transfer process should be the rate-limiting step, assuming a transfer coefficient of $0.3 < \alpha < 0.7$.[21] The influence of scan rate on the oxidation current of AA was also made (inset of Fig. 5A). There is a linear correlation between the anodic current and the scan rate in the range of 0.01–0.1 Vs^{-1} with a correlation coefficient of 0.9898, suggesting that the kinetics of the overall process are controlled by an adsorption process.[22]

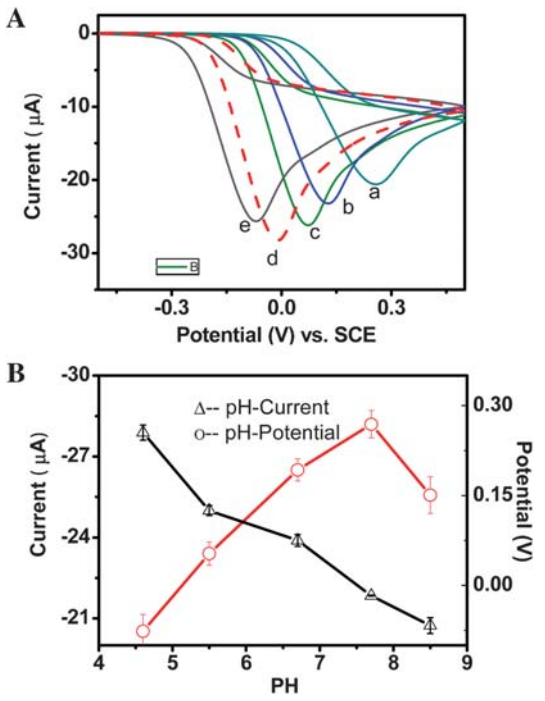

Fig. 4 Cyclic voltammograms of the NBE electrode in 0.5 mM AA at (a) pH 4.6; (b) 5.5; (c) 6.7; (d) 7.7; and (e) 8.5 solutions at the NBE electrode (from right to left) (A), and the dependences of the AA peak current and redox potential on the PBS solution pH (B) with a scan rate of 0.1 V/s.

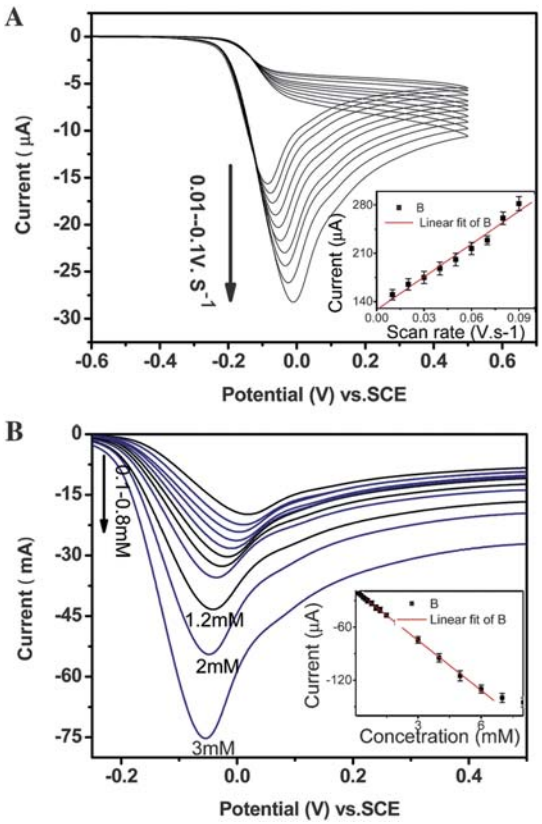

Fig. 5 (A) Cyclic voltammograms of the NBE electrode in 0.1 M PBS solution (pH = 7.7) containing 0.5 mM AA at different scan rates (0.01–0.1 V/s); inset (A) is a linear relationship between the anodic current and scan rate. (B) Cyclic voltammograms of the NBE electrode in 0.1 mM PBS solutions (pH = 7.7) at a scan rate of 0.1 V/s. Curves were obtained using different concentrations of AA (0.1–0.8 mM, step is 0.1 mM; 1.2 mM, 2 mM, and 3 mM); inset (B) is the linear fitting program of the oxidation peak currents with the AA concentrations.

A series of differential pulse voltammetry (DPV) curves was recorded at various concentrations of AA to determine its calibration curve. The response of the NBE electrode to AA was found to increase with increasing AA concentration. Fig. 5B shows the DPV curves recorded on the NBE electrode in the presence of various AA concentrations in the range of 0.1–3 mM. The inset in this figure represents the calibration curve for the determination of AA at the NBE electrode. Linear dependency could be witnessed between the current response and concentration of AA in the range of 0.017–6 mM with a sensitivity and correlation coefficient of 17.53 μA mM^{-1} and 0.9965. The detection limit was 6.4 μM at a signal-to-noise ration of 3. Compared with other AA sensors, the NBE exhibits a lower detection limit and a comparable linear range.[2–16] In particular, the proposed method avoids using diffusion electron transfer mediators for the determination of AA, which is necessary for traditional non-enzyme-based biosensors, and realizes a reagentless AA biosensing.

Considering that the high electrocatalytic performance and simple fabrication method make the as-prepared NBE electrode a good electrochemical sensing platform for the amperometric determination of AA, the effect of applied potential on the steady-state current was investigated under stirred conditions to obtain the maximum catalytic current (see inset of Fig. 6A). The results indicated that with the applied potential shifting from −0.1 to 0.4 V, the steady-state current rapidly increased until it reached a maximum value at −0.013 V. Therefore, −0.013 V was identified as the optimum applied potential for the amperometric detection of AA. Fig. 6 shows the amperometric responses of the NBE electrode to successive injection of AA at low concentrations. The time required to reach 95% of the maximum steady-state current was less than 8 s, indicating a fast response which was mainly due to the excess electroactive sites provided by the $Cu_4(OH)_6SO_4$ nanostructures as well as the good conductivity between the film and the GCE substrate. The much enhanced sensitivity and a fast response can be explained in two aspects. On the one hand, the $Cu_4(OH)_6SO_4$ nanostructures result in the formation of three 3D networks, one consisting of the interconnected nanotubes, and the other two consisting of the hollow inner and the porous wall of the nanotube while the former is also blended with macropores of the powder coating. Such a nanostructure is more favorable for providing a large contact area between the sensing materials and sensed species than the non-hierarchical nanoparticle or bulk $Cu_4(OH)_6SO_4$ powders. Furthermore, due to the small size of the nanotubes, the charge distribution on the surface may lead to less resistance to the diffusion of probe ions onto the electrode surface than that of the bulk $Cu_4(OH)_6SO_4$. Thus, the $Cu_4(OH)_6SO_4$ nanostructure coating can promote the transportation and accessibility of target molecules more effectively and facilitate the transfer of electrons or signals, which is the key to the much enhanced sensitivity and lowered non-faradaic behavior.

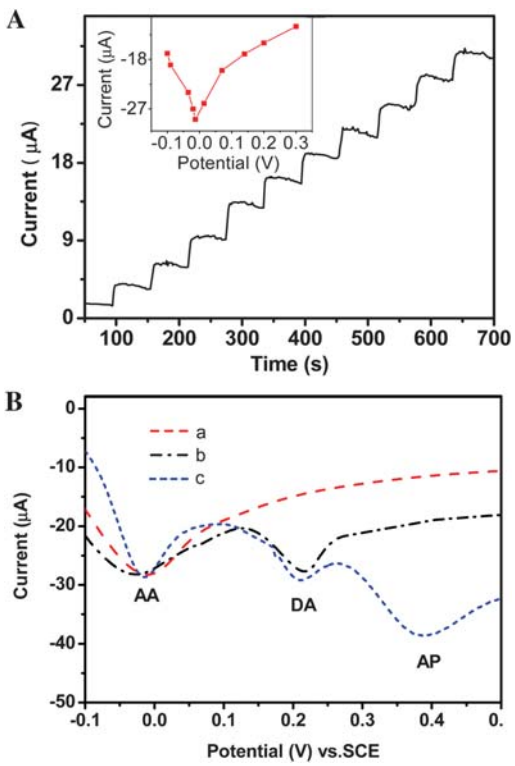

Fig. 6 (A) Amperometric responses of the NBE electrode at an applied potential of −13 mV to the successive addition of 0.5 M AA in a stirred 0.1 M, pH 7.7 PBS solution; inset: calibration curve. (B) The DPVs for the NBE electrode in 0.1 M PBS solutions (pH 7.7) with a 0.1 V/s scan rate: (a) in the presence of 0.5 mM AA; (b) in the presence of 0.5 mM AA and 0.5 mM DA; and (c) in the presence of 0.5 mM AA, 0.5 mM DA and 0.5 mM AP.

An important analytical parameter for a biosensor is its ability to discriminate between the interfering species commonly present in similar physiological environment and the target analyte. Voltammetric response of the NBE electrode was examined in the presence of some electroactive interfering substances like DA and AP at both normal physiological levels as Fig. 6B shows. DPVs were taken for the oxidation of AA (0.5 mM) after the addition of 0.5 mM DA and 0.5 mM AP. As can be seen the obtained current in the absence of any interferent was 28.2 μA with the NBE electrode. After the addition of 0.5 mM DA and 0.5 mM AP successively, two new anodic peaks appeared one after another, corresponding to DA and AP oxidation respectively. The steady-state current to AA was increased to 101% and 102% of the original response by the addition of 0.5 mM DA and 0.5 mM AP successively. It is noted that the anodic peak currents of AA change little with the intervention of DA and AP, and the anodic peak potential for AA, DA and AP were all distinguishable. There was no obvious interference in the measure of the electrode. *Compared with other copper nanoparticles such as Cu_2O/$Cu(OH)_2$/copper complex modified electrodes,*[23–25] *such $Cu_4(OH)_6SO_4$ rod-like nanomaterials provide comparable linear range, sensitivity, selectivity as well as a simpler fabrication process and lower cost.*

The operational stability of the NBE electrode was investigated in a continuous operation mode. The data from the circular experiments revealed high catalysis ability. While not in use, the NBE electrodes were stored in nitrogen. The storage stability was examined at the same NBE electrode. In the repeated measurements in consecutive months, the response to the oxidation of the substance with the same concentration at the optimum potential was maintained at 99% of the initial values. The good long-term stability of the NBE could be attributed to its structure stability.

Conclusions

In summary, $Cu_4(OH)_6SO_4$ nanorods were synthesized and found to possess an intrinsic electrocatalytic activity for the fabrication of AA sensors. Due to the intrinsic structure stability, good orientation and high specific surface, the NBE electrode showed both high selectivity and sensitivity in the determination of AA from DA and AP. The good analytical performance, low cost and straightforward preparation method may lead us to possible breakthroughs in designing enzymeless AA sensing devices that realize innovative and powerful detection based on this new electrode material.

Acknowledgements

This work was supported by the National Natural Science Foundation of China (No. 50902007), the Natural Science Foundation of Jiangsu Province (SBK201022775), the Natural Science Foundation of Jiangsu Universities (No. 09KJB430005), the Specialized Research Fund for the Qinglan Engineering Program of Jiangsu province, and the Fundamental Research Funds for the Central Universities (No. YMF1002016).

References

1 O. Arrigoni and C. D. Tullio, Ascorbic acid: more than just an antioxidant, *Biochim. Biophys. Acta, Gen. Subj.*, 2002, **1569**, 1–9.
2 H. W. Park, S. M. Alam, S. H. Lee, M. M. Karim, S. M. Wabaidur, M. Kang and J. H. Choi, Optical ascorbic acid sensor based on the fluorescence quenching of silver nanoparticles, *Luminescence*, 2009, **24**, 367–71.
3 I. J. Chen and E. Lindner, Lab-on-chip flow injection analysis system without an external pump and valves and integrated with an in line electrochemical detector, *Anal. Chem.*, 2009, **81**, 9955–9960.
4 A. Barberis, G. Bazzu, G. Calia, G. M. Puggioni, G. G. Rocchitta, R. Migheli, M. Schirra, M. S. Desole and P. Serra, A New ultralow-cost telemetric system for a rapid electrochemical detection of vitamin C in fresh orange juice, *Anal. Chem.*, 2010, **82**, 5134–5140.
5 M. Bener, M. Zyrek, K. Gl and R. Apak, Development of a Low-cost optical sensor for cupric reducing antioxidant capacity measurement of food extracts, *Anal. Chem.*, 2010, **82**, 4252–4258.
6 U. Guth, W. Vonau and J. Zosel, Recent developments in electrochemical sensor application and technology-a review, *Meas. Sci. Technol.*, 2009, **20**, 042002-1–042002-14.
7 Aihua Liu, Towards development of chemosensors and biosensors with metal-oxide based nanowires or nanotubes, *Biosens. Bioelectron.*, 2008, **24**, 167–177.
8 A. P. O'Mullane, J. Zhang, W. Surareungchai, M. Somasundrum and A. M. Bond, Investigation of mediated oxidation of ascorbic acid by ferrocenemethanol using large-amplitude fourier transformed ac voltammetry under quasi-reversible electron-transfer conditions at an indium tin oxide electrode, *Anal. Chem.*, 2008, **80**, 6515–6525.
9 R. Aguilar, M. M. D'avila, M. P. Elizalde, J. Mattusch and R. Wennrich, Capability of a carbon-polyvinylchloride composite electrode for the detection of dopamine, ascorbic acid and uric acid, *Electrochim. Acta*, 2004, **49**, 851–859.
10 L. Xiao, G. G. Wildgoose and R. G. Compton, Exploring the origins of the apparent "electrocatalysis" observed at C_{60} film-modified electrodes, *Sens. Actuators, B*, 2009, **138**, 524–531.
11 M. N. Zhang, K. Liu, L. Xiang, Y. Q. Lin, L. Su and L. Q. Mao, Carbon nanotube-modified carbon fiber microelectrodes for *in vivo* voltammetric measurement of ascorbic acid in rat brain, *Anal. Chem.*, 2007, **79**, 6559–6565.
12 L. N. Wu, X. J. Zhang and H. X. Ju, Detection of NADH and ethanol based on catalytic activity of soluble carbon nanofiber with low overpotential, *Anal. Chem.*, 2007, **79**, 453–458.
13 M. N. Zhang, K. P. Gong, H. Z. Zhang and L. Q. Mao, Electrostatic layer-by-layer assembled carbon nanotubes for selective determination of dopamine in the presence of ascorbic acid, *Biosens. Bioelectron.*, 2005, **20**, 1270–1276.
14 L. Zhang, Y. G. Sun and X. Q. Lin, Separation of anodic peaks of ascorbic acid and dopamine at an ct-alanine glassy carbon electrode, *Analyst*, 2001, **126**, 1760–1763.
15 S. A. Kumar, P. Hs. Lo and S. M. Chen, Electrochemical selective determination of ascorbic acid at redox active polymer modified electrode derived from direct blue 71, *Biosens. Bioelectron.*, 2008, **24**, 518–523.
16 S. R. Hou, N. Zheng, H. Y. Feng, X. J. Li and Z. B. Yuan, Determination of dopamine in the presence of ascorbic acid using poly(3,5-dihydroxy benzoic acid) film modified electrode, *Anal. Biochem.*, 2008, **381**, 179–184.
17 F. C. Hawthorne, L. A. Groat and R. K. Eby, Antlerite, $Cu_4(OH)_6SO_4$, a heteropolyhedral wallpaper structure, *Can. Mineral.*, 1989, **27**, 205–209.
18 S. Merlino, N. Perchiazzi and D. Franco, Brochantite, $Cu_4(OH)_6SO_4$: OD character, polytypism and crystal structures, *Eur. J. Mineral.*, 2003, **15**, 267–275.
19 A. Kaushika, R. Khana, P. Pandeya and B. D. Malhotraa, Iron oxide nanoparticles–chitosan composite based glucose biosensor, *Biosens. Bioelectron.*, 2008, **24**, 676–683.
20 Y. Zhuo, P. X. Yuan, R. Yuan, Y. Q. Chai and C. L. Hong, Bienzyme functionalized three-layer composite magnetic nanoparticles for electrochemical immunosensors, *Biomaterials*, 2009, **30**, 2284–2290.
21 L. Zhang and S. Dong, The electrocatalytic oxidation of ascorbic acid on polyaniline film synthesized in the presence of camphorsulfonic acid, *J. Electroanal. Chem.*, 2004, **568**, 189–194.
22 J. Davis, M. Moorcroft, S. J. Wilkins, R. G. Compton and M. F. Cardosi, Electrochemical detection of nitrate and nitrite at a copper modified electrode, *Analyst*, 2000, **125**, 737–742.
23 S. Chen, J. Liu and R. Thangamuthu, Preparation, characterization and electrocatalytic studies on copper complex dye film modified electrodes, *Electroanalysis*, 2007, **19**, 1429–1436.
24 Z. Dursun and G. Nisli, Voltammetric behavior of copper(I)oxide modified carbon paste electrode in the presence of cysteine and ascorbic acid, *Talanta*, 2004, **63**, 873–878.
25 A. Safavi, N. Maleki, E. Farjami and F. A. Mahyari, Simultaneous electrochemical determination of glutathione and glutathione disulfide at a nanoscale copper hydroxide composite carbon ionic liquid electrode, *Anal. Chem.*, 2009, **81**, 7538–7543.

